Predicting order-disorder phase transitions of O/Pd(111) from *ab initio* Wang-Landau Monte Carlo calculations

S. Piccinin[1,2] and C. Stampfl[2]
[1]*CNR-IOM, DEMOCRITOS National Simulation Center, Theory@Elettra Group, Trieste, Italy*
[2]*School of Physics, The University of Sydney, Sydney, New South Wales 2006, Australia*
(Received 12 January 2010; revised manuscript received 26 February 2010; published 13 April 2010)

We study the O/Pd(111) system using a lattice-gas Hamiltonian where the many-body interactions among the oxygen adsorbates are derived from a series of density-functional-theory calculations. Through Monte Carlo simulations that employ the Wang-Landau algorithm, we use this Hamiltonian to predict the order-disorder phase-transition temperature as a function of oxygen coverage. We find that oxygen forms ordered $p(2\times2)$, $(\sqrt{3}\times\sqrt{3})R30°$ and $p(2\times1)$ structures, in agreement with the zero-temperature convex hull, which undergo a continuous transition to a disordered phase upon increasing the temperature. The transition temperature versus coverage curve displays peaks around the coverages corresponding to the formation of the $p(2\times2)$ and $p(2\times1)$ ordered structures, similar to what has been found from experimental and theoretical studies of the O/Pt(111) and O/Ru(0001) systems.

DOI: 10.1103/PhysRevB.81.155427 PACS number(s): 68.35.Rh, 31.15.E−, 68.43.De

I. INTRODUCTION

The oxidation of CO to CO_2 over transition metal surfaces, in particular those belonging to the platinum group, is one of the most investigated catalytic processes, as it is a fundamental surface reaction with important applications in several industrial fields, such as in the reduction in pollutants contained in automotive exhausts. If atomic oxygen adsorbed on these metal surfaces is exposed to CO gas, the metal can catalyze the formation of CO_2 through a Langmuir-Hinshelwood mechanism, in which both reactants are adsorbed on the surface before combining to form CO_2.[1,2] It has been observed that the activation energy of this reaction depends on the coverage of adsorbates, suggesting that lateral interactions between the adsorbates are significant.[3] In the case of Pt(111) it was shown that while at low CO coverage the reaction takes place between isolated O atoms and the adsorbed CO, at higher coverage the reaction site switches to the periphery of $O(2\times2)$ islands.[4] Lateral interactions seem to play an even larger role in the case of Pd(111).[5] Here it was observed that, upon exposure to CO, the $p(2\times2)$ oxygen islands formed by the initial adsorption of oxygen on the metal surface, are compressed into $(\sqrt{3}\times\sqrt{3})R30°$ domains and finally into $p(2\times1)$ domains. This is different to the behavior of Pt(111), where no phase transition is observed in the adsorbed O islands. These structural rearrangements of the oxygen overlayer have profound effects on the reactivity toward the formation of CO_2 over Pd(111): While the $p(2\times2)$ phase is unreactive in the 190–320 K temperature range, the $(\sqrt{3}\times\sqrt{3})R30°$ phase displays half-order kinetics with respect to the oxygen coverage, suggesting that the reaction site is at the periphery of the O islands. For the $p(2\times1)$ phase, on the other hand, the reaction is first order, implying that the reaction proceeds uniformly over the O islands and suggesting that CO is adsorbed inside the O domains. By monitoring the temperature dependence of the rate constant, Nakai *et al.*[5] estimated that the activation energies for the active phases are 0.04 ± 0.02 eV for the $(\sqrt{3}\times\sqrt{3})R30°$ phase and 0.29 ± 0.03 eV for the $p(2\times1)$.

In light of the above observations, it is clear that lateral interactions between adsorbates can play a crucial role in catalytic processes such as CO oxidation. The switching of the reaction site induced by the adsorbate-adsorbate interaction alters the spatial distribution of the reactants and hence the reaction paths. Having a detailed knowledge of these interactions and quantifying their effect is therefore of great importance for heterogeneous catalysis on metal surfaces. Traditionally these quantities have been estimated empirically from experimental data, by assuming pairwise interactions and fitting temperature-programmed desorption and low-energy electron-diffraction (LEED) measurements.[6] An alternative approach is to extract them from first-principles calculations, by assuming a lattice representation of the system and writing its Hamiltonian (lattice-gas Hamiltonian, LGH) in terms of many-body interactions computed theoretically, typically employing density-functional-theory (DFT) calculations. This approach has already been used successfully in the past, for example, to predict the temperature-programmed desorption[7] and the surface phase diagram[8] of the O/Ru(0001) system as well as the phase diagram of alloys.[9,10]

Here, as the initial step toward a detailed understanding of the role played by lateral interactions in CO oxidation over Pd(111), we restrict ourselves to the presence of just one type of adsorbate, oxygen, and study the O/Pd(111) system using a LGH parametrized with DFT energetics. We validate the LGH expansion by comparing the ground-state curve obtained with this approach with that obtained from full DFT calculations. We then predict the order-disorder phase-transition critical temperature as a function of the O coverage through Monte Carlo (MC) simulations using the Wang-Landau algorithm, which is an importance sampling method that presents considerable advantages over the more commonly used Metropolis method.

 ©2010 The American Physical Society

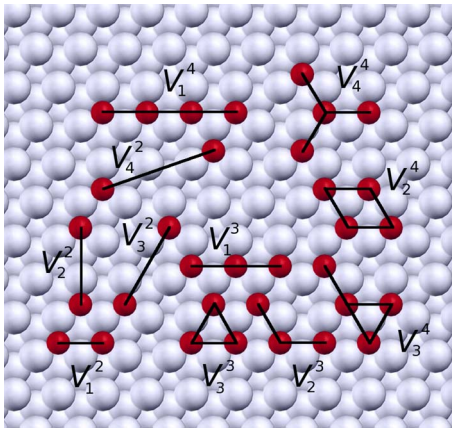

FIG. 1. (Color online) Top view of the O/Pd(111) system, showing the pool of lateral interactions between O adsorbates. Light gray spheres represent Pd atoms, small dark spheres O atoms.

II. METHOD

A. Lattice-gas Hamiltonian parametrized with DFT calculations

In the LGH approach one assumes that the system can be described by the adsorbates occupying a set of points i in a lattice. Any configuration of the system is therefore determined by specifying the occupations of all the lattice sites. Indicating with n_i the occupation of site i, which can be either 0 if the site is empty or 1 if it is occupied, one can write the Hamiltonian of the system as

$$H^{\mathrm{LGH}} = V^1 \sum_i n_i + \sum_{m=1}^{r} V_m^2 \sum_{\langle ij \rangle_m} n_i n_j + \sum_{m=1}^{q} V_m^3 \sum_{\langle ijk \rangle_m} n_i n_j n_k + \cdots . \tag{1}$$

Here V^1 is the one-body term which accounts for the adsorption energy of an isolated adsorbate, V_m^2 are the two-body, or pair, interactions (we consider r possible pair interactions, with $m=1$ corresponding to nearest-neighbor interactions, $m=2$ second nearest-neighbor interactions, and so on), V_m^3 are the three-body, or trio, interactions (we consider q possible trio interactions) and so forth. While in principle the cluster expansion [Eq. (1)] includes an infinite number of terms and summations, in practice it can be truncated since higher-order and longer-distance interactions are typically found to be negligible compared to lower-order and shorter-distance interactions. To select which terms to include in the expansion and to evaluate the accuracy of such an expansion we use the leave-one-out cross validation[11] (LOO-CV) approach described below. The pool of interactions considered in this work are shown in Fig. 1. They include four types of two-body, three types of three-body, and four types of four-body interactions.

The DFT calculations are performed using the generalized gradient approximation (GGA) of Perdew-Burke-Ernzerhof (PBE) (Ref. 12) for the exchange and correlation functional. We use ultrasoft pseudopotentials[13,14] for the electron-ion interactions, including scalar relativistic effects. The Kohn-Sham wave functions are expanded in plane waves with an energy cutoff of 27 Ry (200 Ry for the charge-density cutoff). To sample the Brillouin zone we use the special-point technique,[15] broadening the Fermi surface according to the Marzari *et al.*[16] cold-smearing technique, using a smearing parameter of 0.03 Ry. In the (1×1) surface unit cell, corresponding to the periodicity of clean Pd(111), a 12×12 mesh was used, with only one point in the orthogonal direction. This amounts to 19 **k** points in the irreducible part of the Brillouin zone of the (1×1) surface unit cell. For larger unit cells, the **k**-point mesh is scaled accordingly. All the calculations are performed using the PWSCF code contained in the QUANTUM-ESPRESSO package.[17] The surface is modeled with a slab geometry in which the adsorbates are created on one side of a four-layer Pd slab. The atomic positions of the bottom two layers are kept fixed at the bulk positions while all the other atoms are relaxed until the forces are smaller than 0.001 Ry/au (0.025 eV/Å). A 12 Å vacuum region is found to be sufficient to ensure negligible coupling between periodic replicas of the slab. For the in-plane lattice spacing we use the calculated equilibrium lattice parameter of Pd, $a_0=3.98$ Å. The experimental value for the lattice parameter is 3.89 Å.

We perform DFT calculations for 22 different O/Pd(111) configurations with coverages in the range 1/9 to 1 ML. For each of these systems we compute the average oxygen binding energy, defined as

$$E_b = -\frac{1}{N_{\mathrm{O}}}\left[E^{\mathrm{tot}}_{\mathrm{O/Pd(111)}} - E^{\mathrm{tot}}_{\mathrm{Pd(111)}} - \frac{N_{\mathrm{O}}}{2}E^{\mathrm{tot}}_{\mathrm{O_2}}\right], \tag{2}$$

where N_{O} is the number of O atoms adsorbed on the surface, $E^{\mathrm{tot}}_{\mathrm{O/Pd(111)}}$, $E^{\mathrm{tot}}_{\mathrm{Pd(111)}}$, and $E^{\mathrm{tot}}_{\mathrm{O_2}}$ are the total energies of the metal slab with adsorbed oxygen, the clean metal slab and the oxygen molecule in gas phase, respectively.

In order to construct the LGH we employ the LOO-CV scheme: out of the 22 configurations we select one to be left out of the pool of the remaining 21 configurations. This set is used to obtain the lateral interactions in the LGH by a least-squares fit, where the LGH interactions are chosen as to minimize the error in the prediction of the average oxygen binding energies of the 21 configurations compared to the DFT values. To validate the predictive power of this set of interactions we compute the CV score by calculating the error in determining the average oxygen binding energy of precisely the structure left out of the pool, using the LGH compared to the DFT value, and averaging this error over all the $M=22$ possible choices for the structure to be left out:

$$\mathrm{CV} = \sqrt{\frac{1}{M}\sum_{i=1}^{M}[E_b^{\mathrm{DFT}}(i) - E_b^{\mathrm{LGH}}(i)]^2}. \tag{3}$$

To decide the number and type of interactions to be included in the cluster expansion, we can use the CV score as a measure of its ability to reproduce the DFT energies. We expect a LGH constructed with too few interactions to perform poorly, leading to a high CV score, while the inclusion of too many interactions compared to the size of data set of DFT structures would lead to overfitting, resulting again in a high CV score. Therefore there should be an optimal choice of interactions that minimizes the CV score.

TABLE I. Interaction parameters for O(fcc)/Pd(111). N is the number of terms included in the LGH. All values are in meV.

N	CV	V^1	V_1^2	V_2^2	V_3^2	V_1^3	V_2^3	V_3^3	V_1^4	V_2^4	V_3^4	V_4^4
3	27.0	−1162	280	51								
4	27.2	−1154	267	49							6	
5	25.7	−1154	266	49		4					5	
6	17.0	−1141	244	43	1		21		12			
7	18.0	−1136	242	39	−6	31	30	−49				
8	20.4	−1136	244	39	−6	32	30	−47			−1	
9	24.8	−1139	247	41	−5	33	18	−35			−3	28
10	47.6	−1139	244	41	−5	34	20	−25		−1	−4	28

Once the lateral interactions have been computed and the LGH has been constructed according to the procedure outlined above, we test its reliability by computing the so-called ground-state line (or convex hull) and check whether the LGH can reproduce the DFT results. To this end we define the formation energy as

$$E_f = \Theta[E_{b,\mathrm{O/Pd(111)}} - E_{b,\mathrm{O}(1\times1)/\mathrm{Pd(111)}}], \tag{4}$$

which is a measure of the stability of a structure with respect to phase separation into a fraction Θ of the full monolayer $\mathrm{O}(1\times1)/\mathrm{Pd}(111)$ and a fraction $1-\Theta$ of the clean slab. Plotting this quantity against the coverage we can identify the structures belonging to the convex hull: all the structures whose formation energy is higher than the corresponding value on the convex hull at the same coverage are unstable against phase separation into the two closest structures belonging to the convex hull.

B. Monte Carlo simulations using the Wang-Landau algorithm

Using the LGH parametrized from first-principles calculations, we study the order-disorder phase transition of the O/Pd(111) system as a function of the coverage. This transition can be monitored experimentally by means of LEED but to the best of our knowledge this has not yet been reported in the literature. We will however compare our predictions with available theoretical and experimental results for the O/Ru(0001),[6] O/Pt(111),[18] O/Ni(111),[19] and O/Pd(100) (Refs. 20 and 21) systems.

Since the standard Metropolis algorithm is rather inefficient for studying phase transitions, we employ the Wang-Landau MC algorithm,[22] which has been shown to yield superior performance compared to other algorithms previously employed for this kind of study. Rather than generating directly the canonical distribution at a given temperature $g(E)e^{-E/k_BT}$ (where T is the temperature and k_B the Boltzmann constant) the Wang-Landau algorithm affords the calculation of the density of (configurational) states $g(E)$ via a random walk that produces a flat histogram in energy space. This is obtained by performing the random walk with a probability proportional to the reciprocal of the density of states $1/g(E)$, continuously updating during the simulation an initial guess for the density of states. When a flat histogram is produced one recovers the true $g(E)$, from which all the thermodynamic functions can be computed. For example, one can compute the Helmholtz free energy as

$$F(T) = -k_BT \ln\sum_E g(E)e^{-E/k_BT} = k_BT \ln(Z), \tag{5}$$

where Z is the partition function, the internal energy as

$$U(T) = \langle E\rangle_T = \sum_E Eg(E)e^{-E/k_BT}/Z \tag{6}$$

and the specific heat as

$$C_v(T) = (\langle E^2\rangle_T - \langle E\rangle_T^2)/T^2. \tag{7}$$

In particular, the divergence of the specific heat at the order-disorder transition temperature can be used to monitor the dependence of this quantity on the coverage. We note that, for a specific coverage, a single simulation suffices to obtain $g(E)$ and hence the transition temperature, while in MC studies that employ the Metropolis algorithm, one needs to perform a series of simulations at various temperatures to check the variations in a properly defined order parameter.

III. RESULTS

A. Construction of the LGH

Oxygen is known to adsorb on high coordination sites of close-packed metal surfaces and, in particular, in the case of Pd(111), the preferred adsorption site is the fcc,[23] as for most other fcc metals. Our computed oxygen binding energy at 1/9 ML coverage is 1.151 eV for the fcc site, 0.909 eV for the hcp site, and 0.593 eV for the bridge site. In the following we will therefore only consider the fcc sites as possible adsorption sites. While this is a good approximation at low temperatures, it is possible that at high temperature the hcp and the bridge sites become populated as well. It has been shown, however, that for the O/Pd(100) system the inclusion of the second most favored adsorption site, the bridge site (which is 0.22 eV less favorable than the hollow site), does not play any role in the surface ordering of the adsorbates, at least in the 0–0.35 ML coverage range.[20]

To compute the lateral interactions we use the LOO-CV method outlined in Sec. II A. The results of the fitting procedure are shown in Table I, where we report the values of lateral interactions in meV and the corresponding CV score. There are several features of these sets of lateral interactions

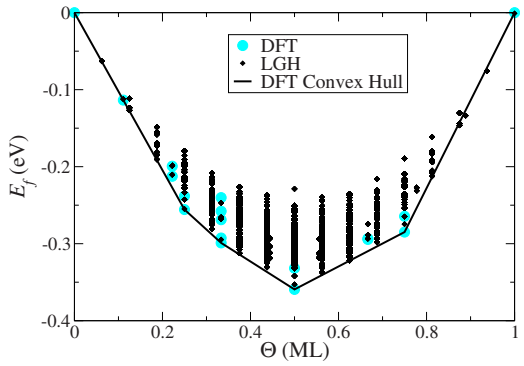

FIG. 2. (Color online) Formation energy versus coverages for the 22 DFT structures (large pale dots) and the LGH formation energies (small black diamonds) computed with the LGH of structures in the (3×3) and (4×4) surface unit cells. The solid line represents the DFT convex hull.

worth discussing. We can see that the on-site one body term V^1 is close to the computed value for the binding energy of oxygen at 1/9 ML coverage, which is reasonable since at that coverage we expect the O atoms to interact weakly among themselves. The magnitude of the two-body terms decreases as the adsorbates are further away and, in general, higher-order terms are smaller than the low-order ones. Again, this is what one would expect since the interactions decay with the distance and many-body terms introduce corrections not already captured by the lower-order terms. We also note that the value of each term is rather constant while varying the total number of interactions in the LGH, which is a sign of the robustness of the cluster expansion. The set with the lowest CV score is the one that includes six lateral interactions, closely followed by the one that includes seven of them. Since the latter is comprised just of one-, two-, and three-body terms we will use in the following this set of lateral interactions for our LGH expansion. The magnitude of the two-body interactions (244, 39, and −6 meV) is remarkably similar to what has been found for the O/Pt(111) system (238, 39, and −6 meV) (Ref. 18) and for the O/Ru(0001) system (265, 44, and −25 meV).[7] It is also interesting to note that the CV score for the optimal set of parameters (17 meV) is very close to the one obtained for the O/Pd(100) system (16 meV).[20]

As test of the reliability of the LGH expression, we calculate with it the formation energy [see Eq. (4)] for all the possible adsorption configurations of oxygen in the (3×3) and (4×4) surface unit cells of Pd(111) and compare them with the ones obtained from the DFT calculations of the 22 configurations used to build the LGH. Plotting the formation energy E_f versus coverage (see Fig. 2) we can identify the convex hull, i.e., the set of structures that are stable against phase separation into any other pair of structures. The agreement between the DFT and the LGH energies is remarkable, except at very high coverages where the large atomic relaxations of the DFT structures are difficult to capture with a simple LGH on a two-dimensional lattice. The important feature of Fig. 2 is the fact that both the DFT and the LGH calculations predict the same ground-state line, implying the LGH is accurate enough to recover the correct ordering of the adsorbates on the surface. In the low-coverage regime the ground-state line includes the $p(2\times2)$ and the $(\sqrt{3}\times\sqrt{3})R30°$ structures, in agreement with experimental findings.[24] The $p(2\times1)$ structure is also observed experimentally but only under special conditions, e.g., when the O/Pd(111) system is exposed to CO gas.[5,24] The only discrepancies are for high coverages beyond 0.9 ML, which however are of limited interest since they are not reachable experimentally, in the low-pressure regime, due to the large O-O repulsion.

Here, we would like to stress how the structures present at the surface of solids are strongly affected by the conditions of the environment in which they operate, i.e., the temperature and partial pressures of the surrounding gas atmosphere.[25] In the case of the O/Pd(111) is has been shown that while in the ultrahigh vacuum regime the adsorption of oxygen leads to the formation of ordered oxygen overlayers, at higher pressure $(5\times10^{-6}$ mbar) and higher temperature (300 °C) a two-dimensional surface oxide can form[26] while bulk oxidation is obtained at even higher oxygen pressure. This has been shown to be the case also for the O/Pd(100) system[27] and for several other transition-metal surfaces such as Ru(110) (Ref. 28) and Ag(111).[29] While these conditions of temperature and pressure are relevant for catalysis, in this work we limit ourselves to the low-pressure regime, therefore neglecting the possibility of the formation of surface oxides. For these conditions, the agreement between the computed and the experimental ground-state line is an indication of the reliability of the DFT calculations for this system, which is obviously a necessary condition for obtaining a meaningful cluster expansion.

B. MC study of the order-disorder phase transition on O/Pd(111)

We apply the LGH derived in the previous section to study the order-disorder phase transition of oxygen adsorbates on the Pd(111) surface. While at low temperature the O/Pd(111) system displays the ordered structures described above, we expect a configurational entropy-driven phase transition to a disordered phase at higher temperatures, similarly to what has been observed for several different adsorption systems.[30] Experiments performed on O/Ru(0001) (Ref. 6) show that the transition temperature strongly depends on the oxygen coverage: it can vary from around 350 K at 0.15 ML to almost 800 K at 0.25 ML. At coverages around 0.4 ML the transition temperature decreases to about 500 K and it later increases to almost 600 K at 0.5 ML. For this system the transition temperature has therefore two peaks, one at 0.25 ML and the other at 0.50 ML, where the stable $p(2\times2)$ and $p(2\times1)$ surface structures are formed. Qualitatively, the same behavior was found for the O/Pt(111) system through theoretical simulations similar to the one presented here.[18] Also the O/Ni(111) system forms a stable $p(2\times2)$ structure, which exhibits a pronounced peak in the order-disorder transition temperature versus coverage curve.[19]

To model the order-disorder phase transition for the O/Pd(111) system we use MC simulations employing the Wang-Landau algorithm outlined in Sec. II B. We use a two-

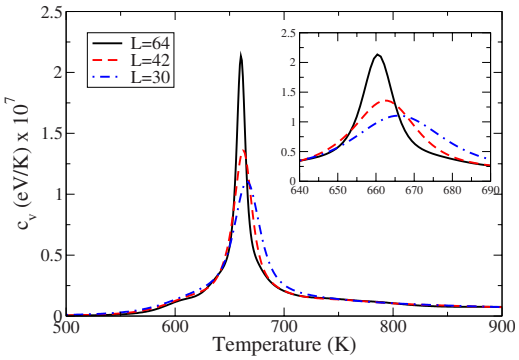

FIG. 3. (Color online) Specific heat, c_v, as a function of temperature for three choices of the size of the lattice. L is the number of points along one of the dimensions of the hexagonal lattice. The oxygen coverage is fixed at 0.25 ML in all three cases. The inset shows an enlargement of the three curves around the region of the peak.

dimensional hexagonal lattice with periodic boundary conditions in which O atoms are allowed to adsorb only on the fcc sites. The Hamiltonian of the system includes seven types of interactions (the on-site energy, three two-body, and three three-body terms, as discussed in Sec. III A). We first fix the coverage at $\Theta=0.25$ ML and study how the order-disorder transition temperature depends on the size of the lattice employed in the simulation. To this end we monitor the divergence of the specific heat [see Eq. (7)], as shown in Fig. 3. For a lattice of dimensions (30×30), (42×42), and (64×64) we obtain a transition temperature $T_c=668\pm16$ K, $T_c=662\pm6$ K, and $T_c=661\pm5$ K, respectively, where the error in T_c is estimated from the full width at half maximum. In the following we will therefore use a (30×30) lattice, which gives transition temperatures converged to within a few K. We also note how the spread of the curves reduces as the dimension of the lattice increases, which is a well-known feature of this kind of lattice simulations.[31]

In Fig. 4 we show the temperature dependence of the free and internal energy for the (64×64) lattice at an oxygen coverage $\Theta=0.25$ ML. The lack of a discontinuity in the internal energy at the transition temperature suggests that the order-disorder phase transition seen here is a continuous

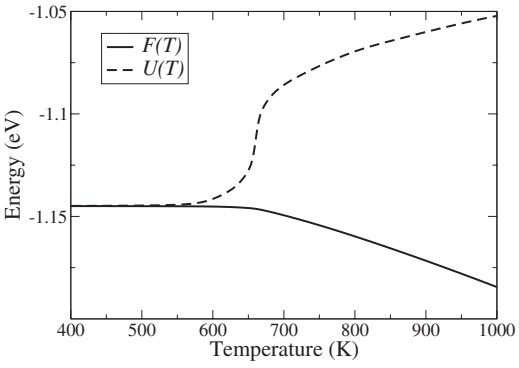

FIG. 4. Free energy $F(T)$ (solid line) and internal energy $U(T)$ (dashed line) as a function of temperature for the (64×64) lattice. The oxygen coverage is $\Theta=0.25$ ML.

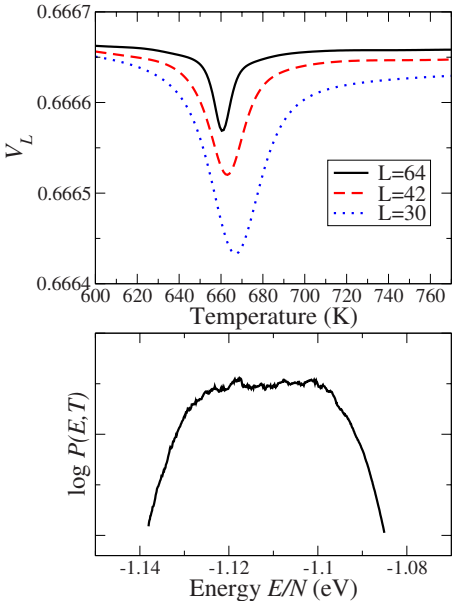

FIG. 5. (Color online) Top panel: V_L as a function of temperature for the (30×30), (42×42), and (64×64) lattices. The oxygen coverage is $\Theta=0.25$ ML. Bottom panel: logarithm of the canonical distribution $P(E,T)=g(E)e^{-E/k_BT}$, at the critical temperature $T=T_c$ as a function of the energy per site E/N. Here we consider the (64×64) lattice, where $T_c=661$ K.

(second-order) phase transition, as already established for similar adsorption systems.[6,18] This is different to what has been found, for example, for the Al-Na surface alloy,[9] which was studied with a theoretical approach similar to the one adopted here. In that case a clear discontinuity in the internal energy at the transition temperature, together with a cusp in the free energy, signaled that the order-disorder phase transition was discontinuous (first order).

Since, however, finite-size effects could smear out the discontinuities seen in first-order phase transitions, we follow Binder and co-workers[32] and monitor the quantity

$$V_L = 1 - \frac{\langle E^4\rangle_L}{3\langle E^2\rangle_L^2}. \tag{8}$$

It has been shown[32] that V_L behaves quite differently for first- and second-order phase transitions: while for the case of first-order phase transitions V_L maintains a prominent minimum at T_c even in the thermodynamic limit $N\to\infty$, for second order-phase transitions the curve flattens out to $V_L=2/3$ as the size of the lattice is increased. As we can clearly see in Fig. 5 the quantity V_L flattens to $V_L=2/3$ as the lattice size is increased, implying that this is a second-order phase transition. We have verified this to be the case also for the order-disorder phase transitions at 0.35 and 0.50 ML. In Fig. 5 we also show the canonical distribution $P(E,T)=g(E)e^{-E/k_BT}$ at the critical temperature for the (64×64) lattice. The lack of a double maximum in the canonical distribution, a characteristic feature of first-order phase transition,[32] is another indication of a continuous phase transition.

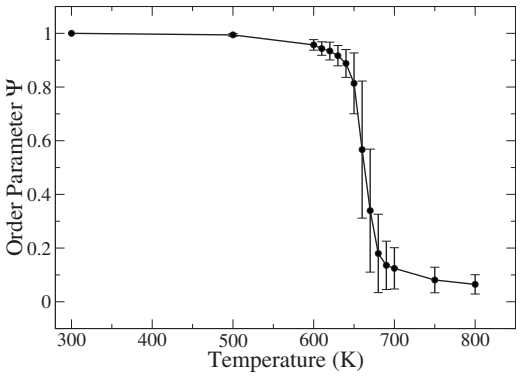

FIG. 6. Dependence of the order parameter for the $p(2\times2)$ structure on the temperature in a MC simulation using the Metropolis algorithm. The coverage is $\Theta=0.25$ ML and we use a (42×42) periodic lattice. The estimated T_c is 663 K. The error bars are given by the rms deviations of the order parameter at each temperature.

As a test of the Wang-Landau algorithm we now compare the predicted transition temperature with the one obtained using the standard Metropolis algorithm under identical simulation conditions [(42×42) lattice at a coverage of 0.25 ML]. With the Metropolis algorithm we need to define an order parameter Ψ that is able to identify the periodic $p(2\times2)$ overlayer and monitor its dependence on the temperature. The transition temperature is defined as the inflexion point of the Ψ versus T curve. We adopt the order parameter proposed by Piercy *et al.*[6] and show in Fig. 6 its dependence on T. The estimated transition temperature is 663 K, in excellent agreement with the result obtained using the Wang-Landau algorithm (662 K). The error bars shown in the figure are the root-mean-square deviation of the order parameter at each temperature.

Having established the reliability of our simulation setup, we now turn to the prediction of the order-disorder transition temperature as a function of the oxygen coverage. This is shown in Fig. 7. We can see two pronounced peaks corresponding to the stable $p(2\times2)$ and $p(2\times1)$ ordered structures, as also observed for the O/Ru(0001) (Refs. 6 and 8) and the O/Pt(111) (Ref. 18) systems. Also the fact that the peak of T_c at 0.25 ML [665, 754, and 670 K for O/Pd(111), O/Ru(0001), and O/Pt(111), respectively] is higher than the

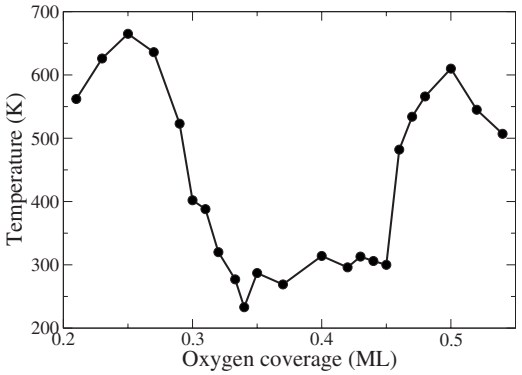

FIG. 7. Order-disorder transition temperature as a function of the oxygen coverage.

one at 0.50 ML [610, 558, and 480 K for O/Pd(111), O/Ru(0001), and O/Pt(111), respectively] is a common feature of all these three systems. In spite of the presence of the $(\sqrt{3}\times\sqrt{3})R30°$ structure in the convex hull, we do not see a peak in Fig. 7 at an oxygen coverage of 1/3 ML. This is similar to what found also for the O/Ru(0001) (Refs. 6 and 8) and the O/Pt(111) (Ref. 18) systems. This might be due to the relatively weak stability of the $(\sqrt{3}\times\sqrt{3})R30°$ structure with respect to decomposition in other structures, as can be seen in the convex hull (see Fig. 2). In spite of this, we verified that for an oxygen coverage of 1/3 ML, below the transition temperature, a $(\sqrt{3}\times\sqrt{3})R30°$ ordered structure is formed. We note here that between the ordered phases which we predict to be stable below the order-disorder curve, we expect to see a first-order phase transition, in analogy to what has been found for the O/Ru(0001) and O/Pt(111) case. Here, however, we did not investigate that portion of the O/Pd(111) phase diagram.

Comparing our results with those obtained by Zhang *et al.*[20] for the O/Pd(100) system with a very similar approach to the one we adopted, we see a similar behavior for the low coverage portion of the phase diagram (the study in Ref. 20 is limited to the 0–0.35 ML range), in particular, the presence of a peak of T_c at 0.25 ML. The smooth variation in T_c with Θ observed experimentally for this system contradicts these findings, but, as already argued in Ref. 20, this could be due to the experimental uncertainty in the precise determination of the oxygen coverage. The direct comparison of the predicted T_c with the experimental measurements allowed Zhang *et al.* to address the ability of DFT-derived lateral interactions that enter the LGH to quantitatively predict this property. The remarkable agreement they found (few tens of K, outside the peak region) strongly supports the validity of this approach to study complex phenomena such as order-disorder phase transitions. It was also found that the major source of uncertainty in the determination of the lateral interactions is the approximate exchange-correlation functional employed to obtain the DFT energetics on which the LGH is parametrized while the other approximations that enter into this type of modeling (finite number of lateral interactions, neglect of vibrational contributions, and neglect of population of other sites besides the most favorable one) have, in comparison, negligible effects. While we do not have the possibility to directly compare our results with experimental measurements, these conclusions established for the O/Pd(100) system may also be expected to hold for O/Pd(111).

The behavior of the order-disorder transition temperature with the oxygen coverage for the O/Pt(111) system reported by Tang *et al.*[18] has remarkable similarities to the O/Pd(111) system studied here: also in that work two large peaks in correspondence with the formation of the ordered $p(2\times2)$ and $p(2\times1)$ structures are seen, with the peak at $\Theta=0.25$ ML having a higher transition temperature compared to the one at $\Theta=0.50$ ML. Moreover, a third ordered structure at a coverage around 0.4 ML was identified, which was shown to be a combination of the $(\sqrt{3}\times\sqrt{3})R30°$ and $p(2\times1)$ structures.

It is worth discussing, at this point, the effect of the approximate nature of the exchange and correlation functional

on the results presented in this work and, in particular, on the order-disorder transition temperature. Zhang *et al.*[20] have compared the lateral interactions for the O/Pd(100) system obtained using the GGA-PBE and the LDA functionals and have shown that, while the on-site energy [V^1 in Eq. (1)] is strongly affected by the type of functional used, the many-body terms are not. The reason for this is the large difference in the GGA vs LDA description of the gas-phase oxygen molecule, which influences all configurations in the same manner and therefore affects only the on-site energy in the LGH, since it is the only term that does not depend on the coverage. Given the fact that in the order-disorder phase transition the number of adsorbates is left unchanged, the transition temperature is unaffected by the value of the on-site energy. As Zhang *et al.* have shown, the transition temperature vs coverage curve is largely unaffected by the change in exchange and correlation functional.

IV. CONCLUSIONS

We have studied, using a Lattice-gas Hamiltonian derived from first-principles DFT calculations, the order-disorder phase transition of the O/Pd(111) system. The lattice-gas Hamiltonian includes up to three-body interactions between the adsorbates, obtained through a leave-one-out cross validation scheme, and its predictive power was tested against the DFT-derived convex hull for this system. In the range of oxygen coverage considered (0.2–0.6 ML) it correctly identified the ordered structures belonging to the convex hull, namely, the $p(2\times2)$ at 0.25 ML, the $(\sqrt{3}\times\sqrt{3})R30°$ at 1/3 ML and the $p(2\times1)$ at 0.5 ML. The Lattice-gas Hamiltonian thus derived was then used in a Monte Carlo scheme with the Wang-Landau sampling, where, at a fixed oxygen coverage, we obtained the density of configurational states by performing a random walk in energy space. This allowed us to compute directly the density of configurational states and hence all the thermodynamic functions of this system. Varying the oxygen coverage we have obtained the coverage dependence of the order-disorder transition temperature. We tested the accuracy and the performance of the Wang-Landau algorithm by benchmarking it against a simulation done using the Metropolis algorithm on an otherwise identical system, finding excellent agreement between the two approaches. We found that the order-disorder phase transition is continuous and that the transition temperature versus coverage curve exhibits two large peaks around oxygen coverages of 0.25 and 0.50 ML, where the $p(2\times2)$ and $p(2\times1)$ phases form. Our theoretical predictions for the O/Pd(111) system show several analogies with the O/Pt(111) and the O/Ru(0001) systems: (i) in all cases the order-disorder phase transition is found to be continuous, (ii) the magnitude of the adsorbate interactions is remarkably similar, and (iii) the peaks in the transition temperature versus coverage curve are an indication of the formation of the ordered structures that are found to lie on the convex hull.

[1] T. Engel and G. Ertl, J. Chem. Phys. **69**, 1267 (1978).
[2] C. T. Campbell, G. Ertl, H. Kuipers, and J. Segner, J. Chem. Phys. **73**, 5862 (1980).
[3] F. Zaera, Prog. Surf. Sci. **69**, 1 (2001).
[4] I. Nakai, H. Kondoh, K. Amemiya, M. Nagasaka, T. Shimada, R. Yokota, A. Nambu, and T. Ohta, J. Chem. Phys. **122**, 134709 (2005).
[5] I. Nakai, H. Kondoh, T. Shimada, A. Resta, J. Andersen, and T. Ohta, J. Chem. Phys. **124**, 224712 (2006).
[6] P. Piercy, K. De'Bell, and H. Pfnür, Phys. Rev. B **45**, 1869 (1992).
[7] C. Stampfl, H. J. Kreuzer, S. H. Payne, H. Pfnür, and M. Scheffler, Phys. Rev. Lett. **83**, 2993 (1999).
[8] J.-S. McEwen, S. H. Payne, and C. Stampfl, Chem. Phys. Lett. **361**, 317 (2002).
[9] M. Borg, C. Stampfl, A. Mikkelsen, J. Gustafson, E. Lundgren, M. Scheffler, and J. N. Andersen, ChemPhysChem **6**, 1923 (2005).
[10] A. Zunger, *Statics and Dynamics of Alloy Phase Transformations*, NATO Advanced Studies Institute, Series B: Physics (Plenum, New York, 1994).
[11] A. van de Walle and G. Ceder, J. Phase Equilib. **23**, 348 (2002).
[12] J. P. Perdew, K. Burke, and M. Ernzerhof, Phys. Rev. Lett. **77**, 3865 (1996).
[13] D. Vanderbilt, Phys. Rev. B **41**, 7892 (1990).
[14] The ultrasoft pseudopotential for Ag, Cu, and O were taken from the PWSCF pseudopotential download page: http://www.pwscf.org/pseudo/html (files: Ag.pbe-d-rrkjus.UPF, Cu.pbe-d-rrkjus.UPF, O.pbe-rrkjus.UPF).
[15] H. J. Monkhorst and J. D. Pack, Phys. Rev. B **13**, 5188 (1976).
[16] N. Marzari, D. Vanderbilt, A. De Vita, and M. C. Payne, Phys. Rev. Lett. **82**, 3296 (1999).
[17] P. Giannozzi *et al.*, J. Phys.: Condens. Matter **21**, 395502 (2009).
[18] H. Tang, A. Van der Ven, and B. L. Trout, Phys. Rev. B **70**, 045420 (2004).
[19] A. R. Kortan and R. L. Park, Phys. Rev. B **23**, 6340 (1981).
[20] Y. Zhang, V. Blum, and K. Reuter, Phys. Rev. B **75**, 235406 (2007).
[21] S.-L. Chang and P. A. Thiel, Phys. Rev. Lett. **59**, 296 (1987).
[22] F. Wang and D. P. Landau, Phys. Rev. Lett. **86**, 2050 (2001).
[23] M. Todorova, K. Reuter, and M. Scheffler, J. Phys. Chem. B **108**, 14477 (2004).
[24] J. Méndez, S. H. Kim, J. Cerdá, J. Wintterlin, and G. Ertl, Phys. Rev. B **71**, 085409 (2005).
[25] C. Stampfl, A. Soon, S. Piccinin, H. Shi, and H. Zhang, J. Phys.: Condens. Matter **20**, 184021 (2008).
[26] E. Lundgren, G. Kresse, C. Klein, M. Borg, J. N. Andersen, M. De Santis, Y. Gauthier, C. Konvicka, M. Schmid, and P. Varga, Phys. Rev. Lett. **88**, 246103 (2002).
[27] E. Lundgren, J. Gustafson, A. Mikkelsen, J. N. Andersen, A. Stierle, H. Dosch, M. Todorova, J. Rogal, K. Reuter, and M. Scheffler, Phys. Rev. Lett. **92**, 046101 (2004).
[28] K. Reuter, C. Stampfl, M. V. Ganduglia-Pirovano, and M. Schef-

fler, Chem. Phys. Lett. **352**, 311 (2002).
[29] A. Michaelides, K. Reuter, and M. Scheffler, J. Vac. Sci. Technol. A **23**, 1487 (2005).
[30] R. Masel, *Principles of Adsorption and Reaction on Solid Surfaces* (Wiley, New York, 1996).
[31] M. E. J. Newman and M. E. J. Newman, *Monte Carlo Methods in Statistical Physics* (Oxford University Press, Oxford, 1999).
[32] M. S. S. Challa, D. P. Landau, and K. Binder, Phys. Rev. B **34**, 1841 (1986).